PROCEEDINGS OF THE ROYAL SOCIETY A

Proc. R. Soc. A (2010) **466**, 407–421
doi:10.1098/rspa.2009.0393
Published online 21 October 2009

On the critical equilibrium of the spiral spring pendulum

BY P. COULLET[1,2], J.-M. GILLI[2,3] AND G. ROUSSEAUX[1,*]

[1]*Laboratoire J.-A. Dieudonné, UMR CNRS-UNS 6621, and* [2]*Institut Robert Hooke de Culture Scientifique, Université de Nice-Sophia Antipolis, Parc Valrose, 06108 Nice Cedex 02, France*
[3]*Institut Non-Linéaire de Nice, Université de Nice-Sophia Antipolis, UMR CNRS-UNS 6618, 1361 route des Lucioles, 06560 Valbonne, France*

Physical systems such as an inverted pendulum driven by a spiral spring, an unbalanced Euler elastica with a travelling mass, a heavy body with a parabolic section and an Ising ferromagnet are very different. However, they all behave in the same manner close to the critical regime for which nonlinearities are prominent. We demonstrate experimentally, for the first time, an old prediction by Joseph Larmor, which states that a nonlinear oscillator close to its supercritical bifurcation oscillates with a period inversely proportional to its angular amplitude. We perform our experiments with a Holweck–Lejay-like pendulum which was used to measure the gravity field during the twentieth century.

Keywords: dynamical system; criticality; nonlinear physics

1. Introduction

Larmor (1893) published a little known paper in which he derived the period of oscillations of a nonlinear oscillator when the linearity is made to vanish. He qualified the related equilibrium position of neutral or critical. He showed that the period of oscillations was inversely proportional to the initial angular amplitude of excursion (see appendix A for a demonstration). Larmor wanted to understand the stability of a solid body resting on a solid surface. The stability of the solid undergoes a pitchfork bifurcation when the centre of gravity G coincides with the centre of curvature O at the point where the body rests and becomes unstable when $G > O$ (figure 1). Geometrically, the point O corresponds to the cusp's extremity of the evolute of the body section.

At the bifurcation, the vertical position loses its stability to the profit of two stable flanking positions, F_1 and F_2, in which the tangents from G to the evolute are vertical. Larmor (1893) derived the nonlinear equation describing the oscillations of a body with the mathematically tractable parabolic section ($y = ax^2$) and whose centre of gravity is at a very short distance c from the cusp O of its evolute. He found that

*Author for correspondence (germain.rousseaux@unice.fr).

Received 25 July 2009
Accepted 21 September 2009

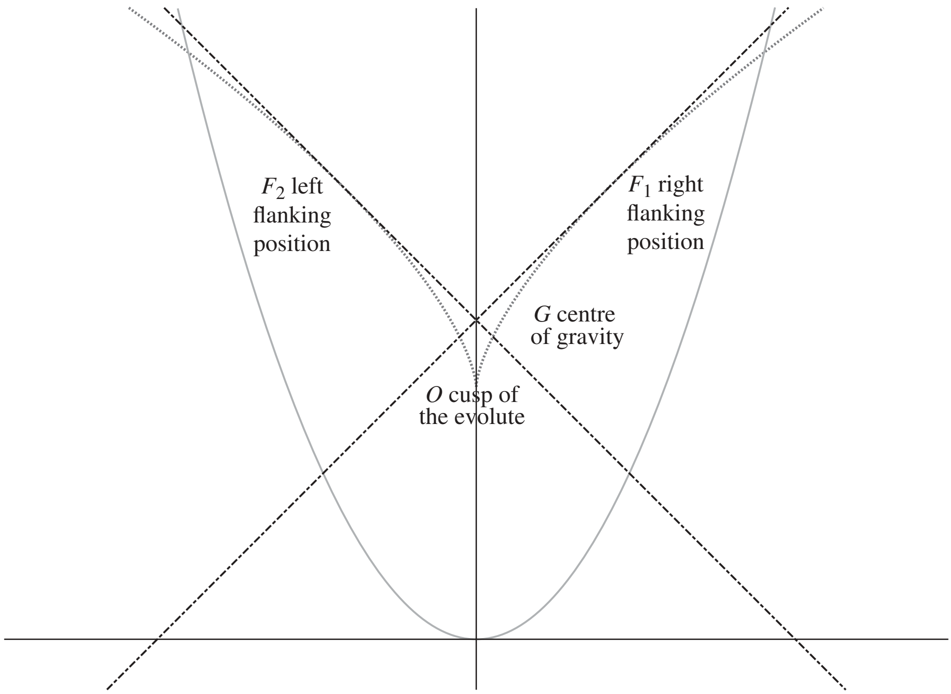

Figure 1. A parabolic solid body resting on a plane surface. Grey curve is the evolute of the parabola: O denotes its cusp. Black lines drawn from the centre of gravity G are tangent to the evolute.

$$\kappa^2\ddot{\theta} = cg\theta - \frac{ag}{4}\theta^3, \tag{1.1}$$

where $\kappa = \sqrt{J/(MA)}$ is the radius of gyration of the solid body of mass M, A is the total cross-sectional area and J the mass moment of inertia. When $c < 0$ and the nonlinearity is negligible, one recovers the equation of a simple pendulum. We can define the equivalent length of the pendulum as $l_{\mathrm{eq}} = \kappa^2/|c|$ and the associated period of oscillations as $T_{\mathrm{body}} = 2\pi\sqrt{l_{\mathrm{eq}}/g} = 2\pi\kappa/\sqrt{|c|g} = 2\pi\sqrt{J/(MA|c|g)}$. Larmor solved the nonlinear equation with the help of complete elliptic integrals of the first and second kinds to derive the law that the frequency of a cubic oscillator close to its pitchfork bifurcation ($c = 0$) is linear with the initial amplitude of excursion when dissipation is negligible.

Here, we study an inverted pendulum as a mechanical analogue of a heavy body rolling on a flat surface. The set-up consists of a rigid bar with a movable mass and a spiral spring. We present the different regimes of oscillations and we focus our attention on the critical regime where linearities are absent and only nonlinearities dictate the behaviour of the pendulum. We point out the analogy with first- and second-order phase transitions 'à la Landau' (Guyon 1975; Charru 1997; Fletcher 1997; Mancuso 2000).

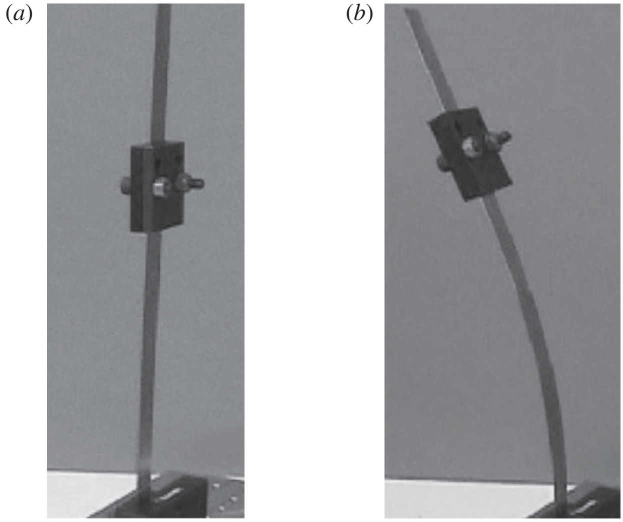

Figure 2. The Euler elastica with a travelling mass: (*a*) $l < l_c$; and (*b*) $l > l_c$.

2. Theoretical context

During the 1930s, the physicist Fernand Holweck and the geophysicist Pierre Lejay developed a gravimeter based on the oscillations of a Euler elastica (figure 2) that is a strip of metal with a mass that can translate along it (Holweck & Lejay 1930, 1931, 1934). The destabilizing effect of gravity is counteracted by the stabilizing elastic torque. The pendulum oscillates around the vertical position of equilibrium $\theta = 0$ for a very long time provided that the set-up is placed within a vacuum chamber so as to minimize the air friction. Holweck & Lejay (1934) were able to carry out campaigns of gravity measurements (e.g. in China) with more than one or two orders of magnitude for the precision than the classical pendulum and with a small, easily transportable and simple experimental apparatus.

From either Euler–Lagrange equations or the balance of moments of momentum, it is straightforward to derive the evolution equation for the deviation angle θ with respect to the vertical direction of a Holweck–Lejay-like pendulum

$$I\ddot{\theta} = mgl \sin\theta - K\theta, \tag{2.1}$$

where I is the mass moment of inertia, m the weight of the translating mass, g the gravity, l the distance of the centre of gravity of the mass to the oscillation axis and K the elastic coefficient of the spiral spring (figure 3).

The equation is invariant under the following symmetries:

(i) time translation: $t \to t + t_0$,
(ii) time reversibility: $t \to -t$,
(iii) space reflection: $\theta \to -\theta$.

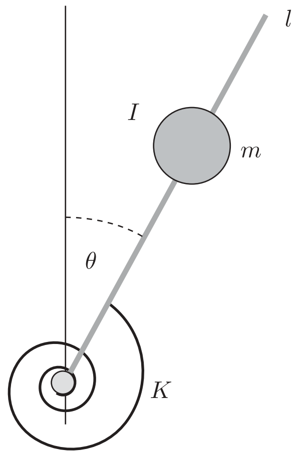

Figure 3. Scheme of the spiral spring inverted pendulum.

(a) *Several behaviours*

We identify four regimes of motion.

(i) $\theta \ll 1,\ K > mgl$ *and* $\omega = \sqrt{(K - mgl)/I}$

The simple linear equation of the usual pendulum is recovered

$$\ddot{\theta} + \omega^2\theta \simeq 0. \tag{2.2}$$

The period of oscillations is

$$T = 2\pi\sqrt{\frac{I}{(K - mgl)}}. \tag{2.3}$$

It is straightforward to evaluate the relative variation of the gravity field as a function of the relative variation of the period to infer the precision of the Holweck–Lejay pendulum

$$\left(\frac{\Delta g}{g}\right)_{\text{H–L}} = \frac{4\pi^2}{T^2}\frac{2l}{g}\frac{\Delta T}{T} = \frac{4\pi^2}{T^2}\left(\frac{\Delta g}{g}\right)_{\text{Classical}}. \tag{2.4}$$

For a period of 1 s, the pendulum of Holweck and Lejay is roughly 40 times more precise than a classical linear pendulum ($I = ml^2$ and $K = 0$; the mass oscillates downwards) whose period is $T_{\text{Classical}} = 2\pi/\omega_0 = 2\pi\sqrt{l/g}$.

(ii) θ *small but finite,* $K > mgl$ *and* $\omega = \sqrt{(K - mgl)/I}$

Taken the smallest nonlinearities into account, we obtain a cubic oscillator

$$\ddot{\theta} + \omega^2\theta + \frac{mgl}{6I}\theta^3 = 0. \tag{2.5}$$

The nonlinear oscillator is of the hard type since the period decreases with the amplitude due to the positive sign of the cubic term. It can be checked readily by deriving the so-called amplitude equation ($\theta = A\,e^{i\omega t} + \text{c.c.} = A\,e^{i\tau} + \text{c.c.}$ where c.c. means the complex conjugate; Cross & Hohenberg 1993):

$$\frac{\partial A}{\partial \tau} = iA + i\frac{mgl}{4I\omega^2}|A|^2 A. \tag{2.6}$$

The amplitude equation is the analogue of the Landau equation for the order parameter in the mean-field theory (Cross & Hohenberg 1993; see below). It is invariant with respect to the symmetries of the initial equation for θ,

(i) $A \to A\,e^{i\phi}$: time translation,
(ii) $A \to -A$: space reflexion,
(iii) $A \to A^*$ and $t \to -t$: time reversibility.

The resultant period taking into account the initial angular amplitude of excursion ($\theta_0 = 2A_0$) due to the influence of nonlinearities is

$$T = \frac{2\pi}{\omega(1 + (mgl/4(K - mgl))A_0^2)} \simeq \frac{2\pi}{\omega}\left(1 - \frac{mgl}{16(K - mgl)}\theta_0^2\right) < \frac{2\pi}{\omega}. \tag{2.7}$$

(iii) *θ small but finite, $K < mgl$ and $\sigma = \sqrt{(mgl - K)/I}$*

$$\ddot{\theta} = \sigma^2\theta - \frac{mgl}{6I}\theta^3. \tag{2.8}$$

We have already studied this equation in another context and we refer the interested reader to Rousseaux (2009).

The equilibrium solutions are $\theta_{eq} = 0$ and $\theta_{eq} = \pm\sqrt{(6I/mgl)}\sigma = \pm\sqrt{6(mgl - K)/mgl}$. One introduces the critical length $l_c = K/mg$ (analogous to the critical temperature T_c in phase transitions, see below) and the latter solutions become, close to the bifurcation,

$$\theta_{eq} \simeq \pm\sqrt{\frac{6(l - l_c)}{l_c}} \approx \pm(l - l_c)^{1/2}. \tag{2.9}$$

The $\frac{1}{2}$ exponent is universal and reminiscent of the Landau mean-field theory for second-order phase transitions: the bifurcation is of the pitchfork type. The space reflection symmetry $\theta \to -\theta$ is broken when the bifurcation occurs. Similarly, the magnetization behaves as $M \approx \pm(T - T_c)^{1/2}$ close to the phase transition in a ferromagnet (Guyon 1975; Charru 1997; Fletcher 1997; Mancuso 2000).

(iv) $K = mgl$

A critical regime appears where linearities are absent

$$\ddot{\theta} = -\frac{mgl}{6I}\theta^3. \tag{2.10}$$

Introducing the short notation for the time derivative $' = \partial_t \sqrt{6I/mgl}$, we have

$$\Theta'' = -\Theta^3. \tag{2.11}$$

Using this rescaling of time, it is straightforward to infer that the period will depend inversely on the initial angular position of the pendulum. Dimensional analysis gives the correct behaviour but is unable to predict the exact numerical value derived in appendix A following Larmor (1893)

$$T = 4\sqrt{\frac{6I}{mgl}}\frac{1.85407}{|\theta_0|}. \tag{2.12}$$

The Holweck–Lejay pendulum and its variants (the present spiral pendulum, the Euler elastica, etc.) enter into a universal class of critical equilibria where linearity vanishes and the period of oscillations is controlled only by nonlinearities.

(b) *The fold catastrophe and its associated cusp*

Pitchfork bifurcations (second-order phase transitions) are not robust when imperfections are introduced (Guyon 1975; Charru 1997; Fletcher 1997; Mancuso 2000); they degenerate into saddle–node bifurcations (first-order phase transitions). Here, the spiral spring is supported on a flat plate. We can introduce an imperfection by inclining the support of a tilting angle α. The equation of evolution becomes (Charru 1997)

$$I\ddot{\theta} = mgl \sin\theta - K(\theta - \alpha). \tag{2.13}$$

The equation is similar to a Newton-like equation

$$I\ddot{\theta} = -\frac{\mathrm{d}U}{\mathrm{d}\theta}, \tag{2.14}$$

with the following potential energy:

$$U(\theta) = -mgl\cos\theta - K\frac{\theta^2}{2} + K\alpha\theta + \text{constant}. \tag{2.15}$$

When $\theta \ll 1$, the potential energy approximates to

$$U(\theta) \simeq mgl\frac{\theta^4}{4!} + (mgl - K)\frac{\theta^2}{2} + K\alpha\theta + \text{constant}'. \tag{2.16}$$

It is analogous to the free energy of an Ising magnet that describes the phase transition from a ferromagnetic to a paramagnetic behaviour (Guyon 1975; Charru 1997; Fletcher 1997; Mancuso 2000)

$$F(M) \simeq a\frac{M^4}{4!} + b(T - T_\mathrm{c})\frac{M^2}{2} + \mu_0 HM + d. \tag{2.17}$$

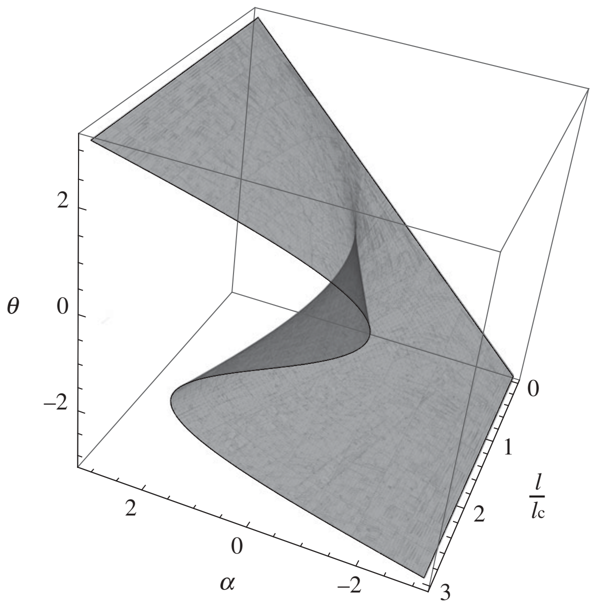

Figure 4. The fold catastrophe: the oscillation angle θ as a function of both the tilting angle α and the reduced length l/l_c.

Table 1. The triple analogy.

solid body	inverted pendulum	Ising ferromagnet
rolling angle, θ	oscillation angle, θ	magnetization, M
distance to the evolute, c	distance to the critical length, $l - l_c$	temperature shift, $T - T_c$
tilting angle, α	tilting angle, α	magnetic field, H
potential energy, U	potential energy, U	free energy, F
equivalent length, l_{eq}	length of the pendulum, l	temperature, T
susceptibility, $\chi_m = \partial\theta/\partial\alpha$	susceptibility, $\chi_m = \partial\theta/\partial\alpha$	susceptibility, $\chi = \partial M/\partial H$

The order parameter of the phase transition is the magnetization M and the control parameter is the temperature T. The magnetic field H induces an additional interaction term linear in the magnetization. We resume the triple analogy in table 1.

For equilibrium positions, the system is described by the implicit equation

$$\alpha = \theta - \beta \sin\theta, \tag{2.18}$$

with $\beta = l/l_c$. If one plots the oscillation angle θ as a function of the reduced length β and the tilting angle α, a fold catastrophe appears (Mancuso 2000) as can be seen easily with the small-angle approximation $\theta \ll 1$ (figure 4)

$$\alpha + (\beta - 1)\theta - \beta\frac{\theta^3}{3!} = 0. \tag{2.19}$$

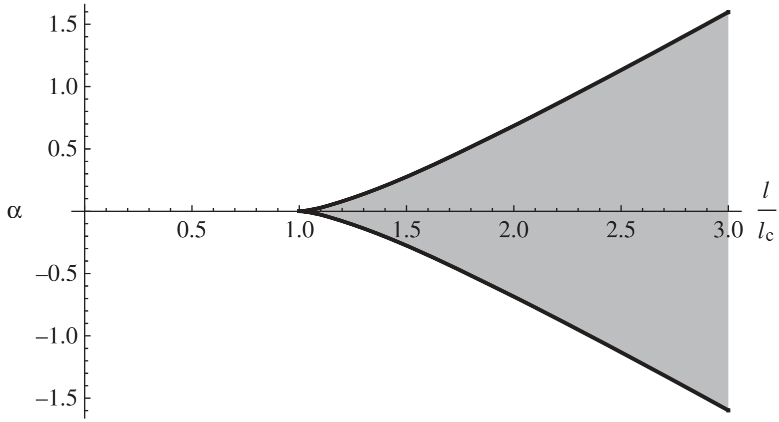

Figure 5. The cusp: the tilting angle α versus the reduced length l/l_c. $\alpha = 0$ and $l = l_c$: pitchfork bifurcation. $\alpha \neq 0$: saddle–node bifurcation on the black lines. Grey region: three fixed points. White region and $\alpha \neq 0$: zero fixed point. White region and $\alpha = 0$: one fixed point.

Similar to the magnetic susceptibility $\chi = \partial M/\partial H$, we introduce the mechanical susceptibility that is a measure of the response of the system to a perturbation/imperfection

$$\chi_m = \frac{\partial\theta}{\partial\alpha} = \frac{1}{1 - \beta\cos\theta}. \tag{2.20}$$

For small oscillation angle $\theta \ll 1$, it is written as

$$\chi_m \simeq \frac{l_c}{l - l_c} \approx (l - l_c)^{-1}. \tag{2.21}$$

One recovers the usual mean-field exponent 1 of Landau theory for the susceptibility as a function of the control parameter. The mechanical susceptibility diverges when θ reaches

$$\theta^* = \cos^{-1}(\beta^{-1}). \tag{2.22}$$

The singularity corresponds to the cusp shape of the projection of the fold catastrophe in the plane ($l/l_c, \alpha$; figure 5)

$$\alpha^* = \cos^{-1}(\beta^{-1}) - \beta(1 - \beta^{-2})^{1/2}. \tag{2.23}$$

3. Numerical validations

For completeness, we display in figures 6 and 7 the different phase spaces ($\dot\theta$ versus θ) corresponding to the regimes that we identified and that describe the behaviour of the inverted pendulum as a function of l. We used a dissipative

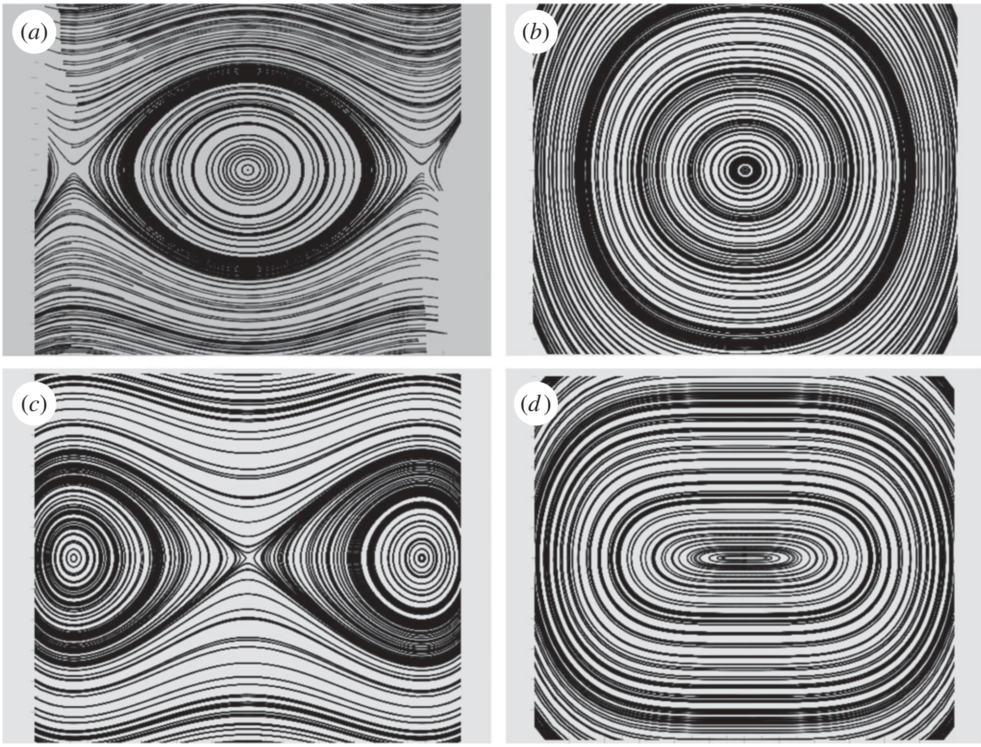

Figure 6. Phase spaces $(\theta, \dot{\theta})$ $(\nu = 0$ and $\alpha = 0)$: (*a*) classical nonlinear pendulum; (*b*) inverted pendulum $l < l_c$; (*c*) inverted pendulum $l > l_c$; and (*d*) inverted pendulum $l = l_c$.

version of the equation with a viscous damping ν and a tilting angle α to treat the general case and to take into account the experimental observed damping due to the friction effects

$$I\ddot{\theta} = mgl \sin\theta - K(\theta - \alpha) - \nu\dot{\theta}. \tag{3.1}$$

For comparison, we recall in figure 6*a* the phase space of the usual nonlinear cubic oscillator. The trajectories are mostly oscillations (closed) when the angles are small. An elliptical heteroclinic trajectory connects the vertical unstable positions. Outside this ellipse, librations characterize the motion of the pendulum. For the inverted pendulum, the behaviour is not the same depending on whether l is superior or inferior to l_c. When $l < l_c$, the trajectories are only oscillations (figure 6*b*). If $l > l_c$, librations appear between the two bifurcated angular positions F_1 and F_2 (figure 6*c*). At criticality, the system hesitates between one and two stable equilibrium positions (figure 6*d*) but only oscillations are observed.

The inclusion of the tilting angle favours one centre of oscillations with respect to the other (figure 7*a*). For a stronger imperfection α, one focus can disappear (figure 7*b*). Viscous friction damps both the oscillations and the librations (figure 7*c*,*d*).

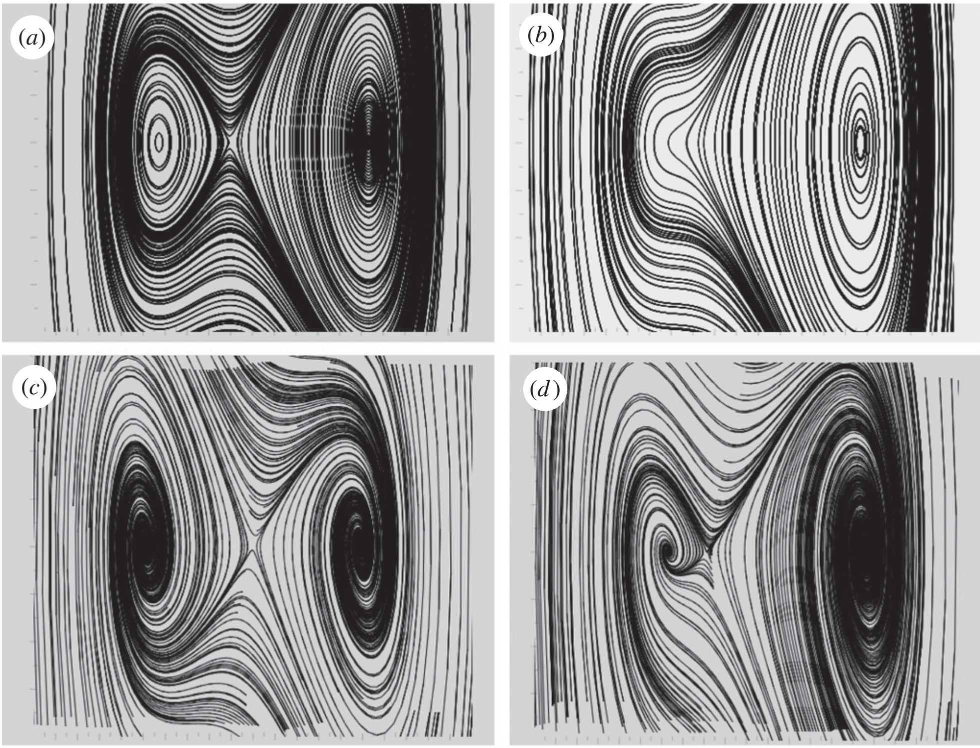

Figure 7. Phase spaces $(\theta, \dot{\theta})$ for the inverted pendulum $l > l_c$: (*a*) $\alpha > 0$, $\nu = 0$; (*b*) $\alpha \gg 0$, $\nu = 0$; (*c*) $\alpha = 0$, $\nu > 0$; and (*d*) $\alpha > 0$, $\nu > 0$.

4. Experimental validations

Experiments have been done with a very simple pendulum that is actually used in our university as a teaching apparatus for students (figure 8; Peters 1995; Charru 1997; Lasic *et al.* 2001; Milotti 2001; Sconza & Torzo 2005).

The spiral spring is handmade, starting from a hardened steel plate, and is characterized by its stiffness $k = 10.8 \times 10^{-3}\,\mathrm{N\,m\,rad^{-1}}$. The position of the brass weight $m = 20.83 \times 10^{-3}\,\mathrm{kg}$ can be varied by screwing it along a threaded rod. The bifurcation length l_c measured from the centre of the pendulum axis to the gravity centre of the brass weight can be obtained by a static method: the equilibrium angle θ varies according to the simple law $\theta/\sin\theta = l/l_c$. As seen in figure 9, it is possible to obtain a value of l_c by the well-known 'extrapolation method' used in the presence of such supercritical transitions. As a matter of fact, it is experimentally very hard to measure directly the critical length by varying the height of the brass weight along the rod, hoping to observe the fall of the rod on either side. Indeed, close to criticality, several equilibrium positions are experimentally observed because of the solid friction that blocks the rod on a position close to the vertical direction. Hence, to infer the critical length, we measure the angle θ as a function of l when $l > l_c$ and one plots $\theta/\sin\theta$ versus l (figure 9).

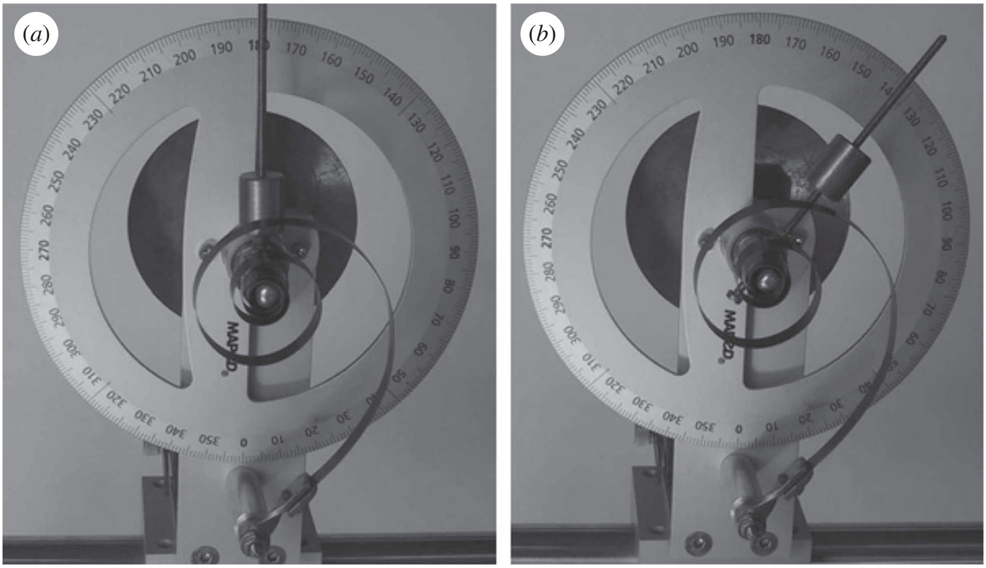

Figure 8. The spiral spring inverted pendulum: (*a*) $l < l_c$; and (*b*) $l > l_c$.

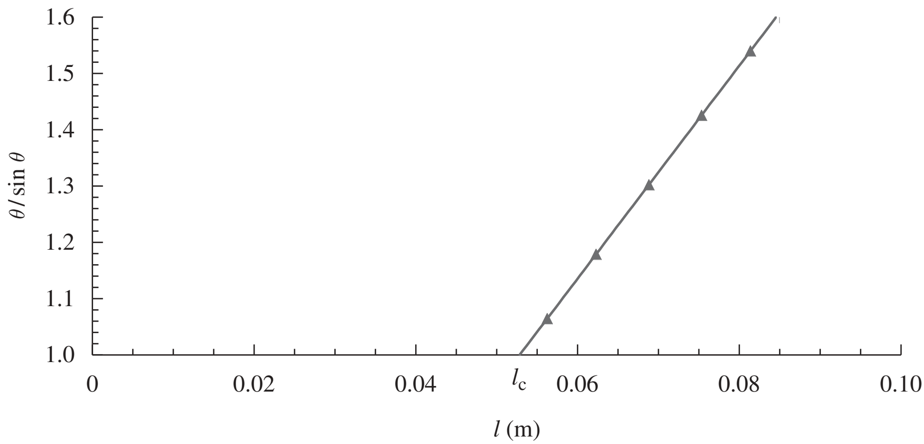

Figure 9. $\theta/\sin\theta$ versus l. One infers the extrapolated value of the bifurcation length $l_c = 53\,\mathrm{mm}$.

The value $l_c = 53\,\mathrm{mm}$ is in good agreement with the one obtained by the dynamical methods used in this paper. The other parts of the oscillating arm are neglected here except the brass wheel ($I = 61.6 \times 10^{-6}\,\mathrm{kg\,m^2}$) associated with the oscillation, which constitutes an important increase in the inertia of the pendulum lowering the importance of friction in the experiment. The only peculiarity to be mentioned concerning this experimental apparatus is the particular care associated with the ball bearing constituting the articulation of the pendulum: grease was removed from it in order to have sufficiently low viscous damping.

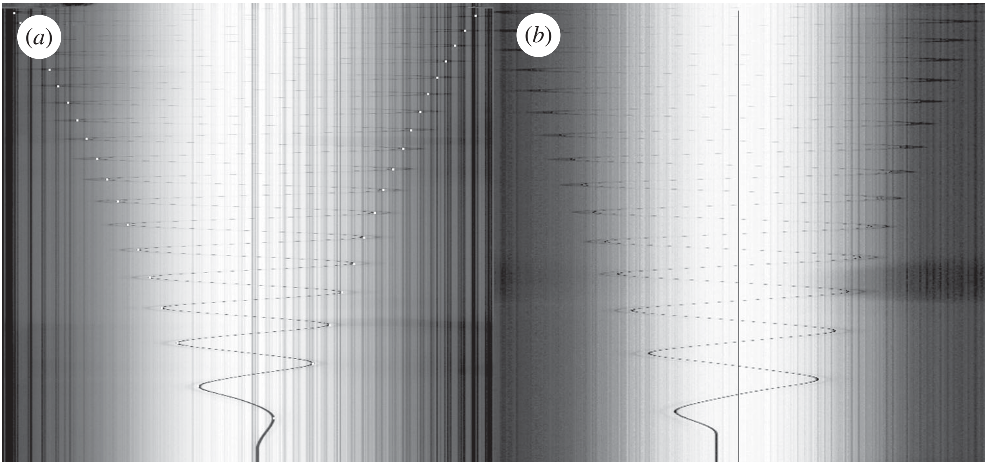

Figure 10. The temporal evolution of the oscillation amplitude: (*a*) $l < l_c$, $\theta_{eq} = 0$; and (*b*) $l > l_c$, $\theta_{eq} \neq 0$. Time is pointing downwards.

Each evolution (θ versus time) was obtained from a video sequence for a given value of l. The films were opened in an Image J stack and treated with a dedicated plug-in that extracts the decreasing oscillation amplitude of the pendulum and allows the measurement of the dependance of the frequency of oscillations with the amplitude since, in one experimental run, the amplitude decreases to zero because of the friction.

Then, the oscillation extrema are dotted (figure 10) and angular positions as well as time coordinates are directly extracted in a table. Subtracting successive values of extrema positions gives us directly the instantaneous period, amplitude and frequency/amplitude dependence curves that are plotted in figure 11.

The spreading extension of the points reported in figures 11 and 12 is associated with the low resolution of the numerical video method used for measurements: a low-definition 25 frames per second camera is used and the Image J extraction software 'unwinds' the angular excursion of the pendulum, giving the decreasing amplitude oscillations shown in figures 11 and 12. The table of values (period versus amplitude) are directly obtained by putting dots on the maxima 'by hands'. The greatest uncertainty and the apparent 'quantization' of the frequency values (particularly visible on the grey upper curve of figure 11) are associated with the low temporal resolution ($\frac{1}{25}$ s) of the method.

Figure 12, corresponding to the frequency/amplitude relation at the critical value l_c, allows the measurement of the slope to be compared with formula (2.12) giving Larmor's prediction for this slope. Taking into account the low precision of the experimental parameters (we minimized, in particular, the inertia), the formula-calculated value $0.523\,\mathrm{Hz\,rad^{-1}}$ appears to be in good agreement with the experimental value $0.457\,\mathrm{Hz\,rad^{-1}}$. We checked experimentally that the period of oscillation tends to infinity when $l = l_c$ for a very small angle θ. This is reminiscent of the well-known criticality slowing down close to a phase transition.

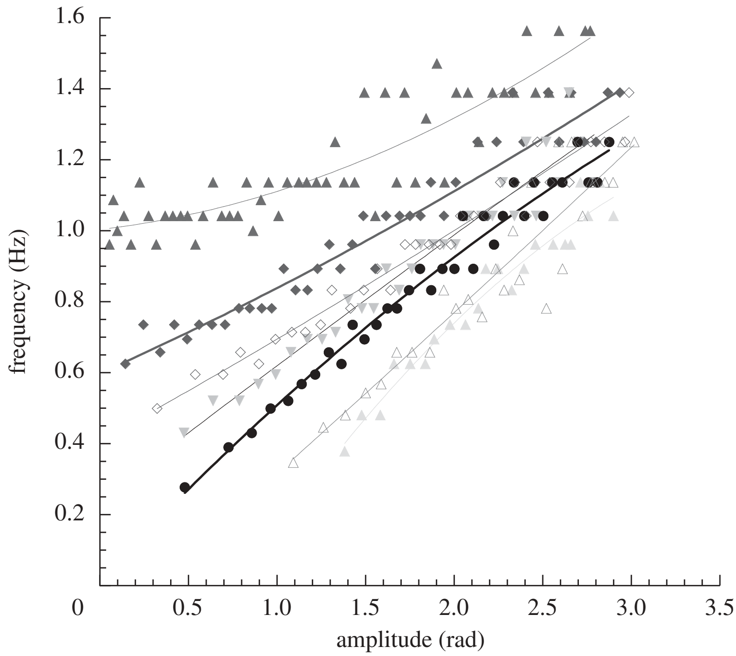

Figure 11. The frequency of oscillations of a Holweck–Lejay-like pendulum as a function of its angular amplitude of excursion for different lengths l. Filled dark grey triangle, $l = 35$ mm; filled black diamond, $l = 43.8$ mm; open diamond, $l = 47.6$ mm; open triangle down, $l = 50$ mm; filled black circles, $l = 52$ mm; open triangle, $l = 55$ mm; filled light grey triangle, $l = 60$ mm.

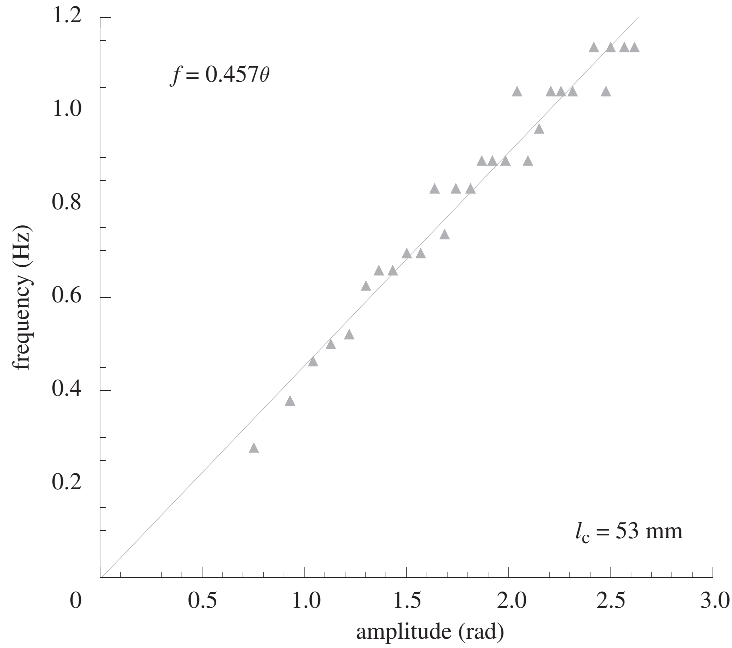

Figure 12. The frequency of oscillations of a Holweck–Lejay-like pendulum as a function of its angular amplitude of excursion at the critical length of 53 mm: the fit gives a 0.457 slope value for the linear dependence of the frequency versus amplitude.

5. Conclusion

We showed that the spiral spring, parabolic heavy body and Holweck–Lejay oscillators belong to the same class of universality as the Ising ferromagnet close to their symmetry-breaking bifurcation. The Larmor's law was confirmed experimentally with a good accuracy. We plan to come back to this problem, this time taking into account the three-dimensional motion of the bob of the inverted pendulum when the system is not constrained to oscillate in a vertical plane. We have already observed a precessing motion of the resulting ellipses.

G.R. would like to thank Marc Monticelli from the Laboratoire Dieudonné for using the software X-Dim with which the phase spaces of figures 6 and 7 were computed and drawn. G.R. and Fernand Holweck spent part of their studies at ESPCI (Ecole Supérieure de Physique et Chimie Industrielles, Paris, France; http://www.espci.fr/) and this paper is a tribute to the great experimental achievements of the ESPCI engineer Holweck. We would like to thank Tomoyuki Nagaya (Oita University) for building the polar extraction Image J plug-in used in the image analysis.

Appendix A

Here, we derive Larmor's (1893) formula for the period of oscillations of a cubic oscillator close to its pitchfork bifurcation. The conservation of energy is written as

$$\frac{1}{2}\left(\frac{\mathrm{d}\theta}{\mathrm{d}\tau}\right)^2 + \frac{\theta^4}{4} = \frac{\theta_0^4}{4}, \qquad \text{(A 1)}$$

where θ_0 is the initial angular amplitude of excursion.

The dimensionless time τ since the launch of the pendulum can be computed with

$$\tau = \int_{\theta_0}^{\theta} \frac{\mathrm{d}\theta}{\sqrt{\theta_0^4/2 - \theta^4/2}}. \qquad \text{(A 2)}$$

Here, we use the following equality:

$$\int \frac{\mathrm{d}\theta}{\sqrt{(1-p\theta^2)(1+q\theta^2)}} = -\sqrt{\frac{1-k^2}{p}} \int \frac{\mathrm{d}\phi}{\sqrt{1-k^2\sin^2\phi}}, \qquad \text{(A 3)}$$

where we introduce $\cos\phi = \sqrt{p}\theta$ and $k^2 = q/(p+q)$.

In our case, $p = q = 1/\theta_0^2$ and $k = 1/\sqrt{2}$. Hence, the period of oscillations of a cubic oscillator close to criticality is (we integrated the previous equality between $\theta_0 = \pi/2$ and $\theta = 0$ to obtain a quarter period)

$$T = 4\sqrt{\frac{6I}{mgl}}\frac{K(1/\sqrt{2})}{|\theta_0|} = 4\sqrt{\frac{6I}{mgl}}\frac{1.85407}{|\theta_0|}, \qquad \text{(A 4)}$$

where 1.85407 is the value of the complete elliptic integral of the first kind $K(k) = \int_0^{\pi/2}(1-k^2\sin^2\phi)^{-1/2}\,\mathrm{d}\phi$ for $k = 1/\sqrt{2}$ as can be checked right away with Mathematica.

For comparison, the period of the classical pendulum taking into account its intrinsic geometrical nonlinearity is written as (Drazin 1993)

$$T = 4\sqrt{\frac{l}{g}}K\left(\sin\left(\frac{\theta_0}{2}\right)\right) \simeq \frac{2\pi}{\omega_0}\left(1 + \frac{1}{16}\theta_0^2\right). \tag{A 5}$$

We recall the Taylor expansion near $k = 0$ of the complete elliptic integral of the first kind

$$K(k) \simeq \frac{\pi}{2}\left(1 + \frac{1}{4}k^2 + \cdots\right). \tag{A 6}$$

References

Charru, F. 1997 A simple mechanical system mimicking phase transitions in a one-dimensional medium. *Eur. J. Phys.* **18**, 417–424. (doi:10.1088/0143-0807/18/6/002)

Cross, M. C. & Hohenberg, P. C. 1993 Pattern formation outside of equilibrium. *Rev. Mod. Phys.* **65**, 851–1112. (doi:10.1103/RevMadPhys.65.851)

Drazin, P. G. 1993 *Nonlinear systems*. Cambridge, UK: Cambridge University Press.

Fletcher, G. 1997 A mechanical analog of first- and second-order phase transitions. *Am. J. Phys.* **65**, 74–81. (doi:10.1119/1.18522)

Guyon, E. 1975 Second-order phase transitions: models and analogies. *Am. J. Phys.* **43**, 877–881. (doi:10.1119/1.9970)

Holweck, F. & Lejay, P. 1930 Un instrument transportable pour la mesure rapide de la Gravité. *C. R. Acad. Sci.* **190**, 1387–1388.

Holweck, F. & Lejay, P. 1931 Perfectionnements à l'instrument transportable pour la mesure rapide de la gravité. *C. R. Acad. Sci.* **192**, 1116–1119.

Holweck, F. & Lejay, P. 1934 Mesures relatives de la Gravité au moyen du Pendule élastique inversé. *J. Observateurs* **17**, 109. http://adsabs.harvard.edu/full/1934JO.....17..109H

Larmor, J. 1893 On critical or 'apparently neutral' equilibrium. *Proc. Camb. Phil. Soc.* IV, Pt VI, 7p.

Lasic, S., Planinsic, G. & Torzo, G. 2001 Torsion pendulum: a mechanical nonlinear oscillator. In *Proc. Int. GIREP Semin. Developing Formal Thinking in Physics, Udinese, Italy, 2–6 September 2001*. Udinese, Italy: Forum Editrice Universitaria Udinese. http://www.padova.infm.it/torzo/torsion_GIREP.pdf

Mancuso, R. V. 2000 A working mechanical model for first- and second-order phase transitions and the cusp catastrophe. *Am. J. Phys.* **68**, 271–277. (doi:10.1119/1.19403)

Milotti, E. 2001 Nonlinear behaviour in a torsion pendulum. *Eur. J. Phys.* **22**, 239–248. (doi:10.1088/0143-0807/22/3/307)

Peters, R. D. 1995 Chaotic pendulum based on torsion and gravity in opposition. *Am. J. Phys.* **63**, 1128–1136. (doi:10.1119/1.18019)

Rousseaux, G. 2009 On the bead, hoop and spring (BHS) dynamical system. *Nonlinear Dyn.* **56**, 315–323. (doi:10.1007/S11071-008-9407-6)

Sconza, A. & Torzo, G. 2005 The torsion pendulum as a tool to study non-linear oscillations and the transition to deterministic chaos. Physics teaching and learning. In *GIREP book of selected papers dedicated to the memory of professor Arturo Loria* (eds M. Michelini & S. Pugliese Jona). Udinese, Italy: Forum Editrice Universitarìa Udinese. http://www.padova.infm.it/torzo/TorsionPendulum.pdf